Journal of Chromatography A, 1490 (2017) 148–155

Contents lists available at ScienceDirect

Journal of Chromatography A

journal homepage: www.elsevier.com/locate/chroma

Full length article

High-throughput quantification of the levels and labeling abundance of free amino acids by liquid chromatography tandem mass spectrometry

Jean-Christophe Cocuron[a,b,1], Enkhtuul Tsogtbaatar[a,1], Ana P. Alonso[a,b,*]

[a] Department of Molecular Genetics, The Ohio State University, 1060 Carmack Road, Columbus, OH, 43210, USA
[b] Center for Applied Plant Sciences, The Ohio State University, 1060 Carmack Road, Columbus, OH, 43210, USA

ARTICLE INFO

Article history:
Received 1 October 2016
Received in revised form 26 January 2017
Accepted 13 February 2017
Available online 16 February 2017

Keywords:
Amino acids
^{13}C-labeling
LC–MS/MS
Mass isotopomer distribution
Multiple reaction monitoring
Metabolic flux analysis

ABSTRACT

Accurate assessment of mass isotopomer distributions (MIDs) of intracellular metabolites, such as free amino acids (AAs), is crucial for quantifying *in vivo* fluxes. To date, the majority of studies that measured AA MIDs have relied on the analysis of proteinogenic rather than free AAs by: i) GC–MS, which involved cumbersome process of derivatization, or ii) NMR, which requires large quantities of biological sample. In this work, the development and validation of a high-throughput LC–MS/MS method allowing the quantification of the levels and labeling of free AAs is described. Sensitivity in the order of the femtomol was achieved using multiple reaction monitoring mode (MRM). The MIDs of all free AAs were assessed without the need of derivatization, and were validated (except for Trp) on a mixture of unlabeled AA standards. Finally, this method was applied to the determination of the ^{13}C-labeling abundance in free AAs extracted from maize embryos cultured with ^{13}C-glutamine or ^{13}C-glucose. Although Cys was below the limit of detection in these biological samples, the MIDs of a total of 18 free AAs were successfully determined. Due to the increased application of tandem mass spectrometry for ^{13}C-Metabolic Flux Analysis, this novel method will enable the assessment of more complete and accurate labeling information of intracellular AAs, and therefore a better definition of the fluxes.

1. Introduction

Organisms are considerably different in their abilities to synthesize amino acids (AAs). For some bacteria, such as *Escherichia coli*, one carbon source (glucose) suffices to produce all the indispensable AAs [1]. Photosynthetic bacteria and plants are even more efficient since they can build all their organic compounds from atmospheric carbon dioxide [2]. However, mammalian cells can only synthesize 11 of the 20 AAs; the remaining nine are essential AAs and must be provided through alimentation. The biosynthesis of AAs uses intermediates from central metabolism whereas their catabolism leads to production of metabolites used by the citric acid cycle as an energy source [3] (Fig. 1). Depending upon the cell type and the organism, AAs are not only used as building blocks for protein biosynthesis, but also as precursors for structural, defense, and regulatory compounds[4–9]. Given that AAs are extensively involved in numerous biochemical reactions; they play a key role in carbon flow throughout the metabolic network.

The common and powerful approach for quantifying *in vivo* carbon distribution is ^{13}C-based metabolic flux analysis (MFA) which involves providing a system of interest with ^{13}C-labeled substrates[10–14]. As the labeled substrates are metabolized, ^{13}C-labeled carbon atoms are incorporated into intermediates and end-products of the metabolic network. The positional distribution and enrichment of labeling in intracellular metabolites can then be determined by either nuclear magnetic resonance spectroscopy (NMR) or mass spectrometry (MS), respectively. Even though NMR is capable of generating a positional labeling information, its sensitivity is limited to compounds of high abundance. In contrast, MS based techniques require much less biological sample and they quantify mass isotopomer distributions (MID) which enable determination of total labeling enrichment within a metabolite. The ^{13}C-labeling data are then integrated into a mathematical model, generating a flux map that describes *in vivo* carbon fluxes [15–22]. Thus, quantification of *in vivo* carbon fluxes at high resolution is

* Corresponding author at: Department of Molecular Genetics, The Ohio State University, 1060 Carmack Road, Columbus, OH, 43210, USA.
E-mail address: alonso.19@osu.edu (A.P. Alonso).
[1] Equal contribution.

http://dx.doi.org/10.1016/j.chroma.2017.02.028

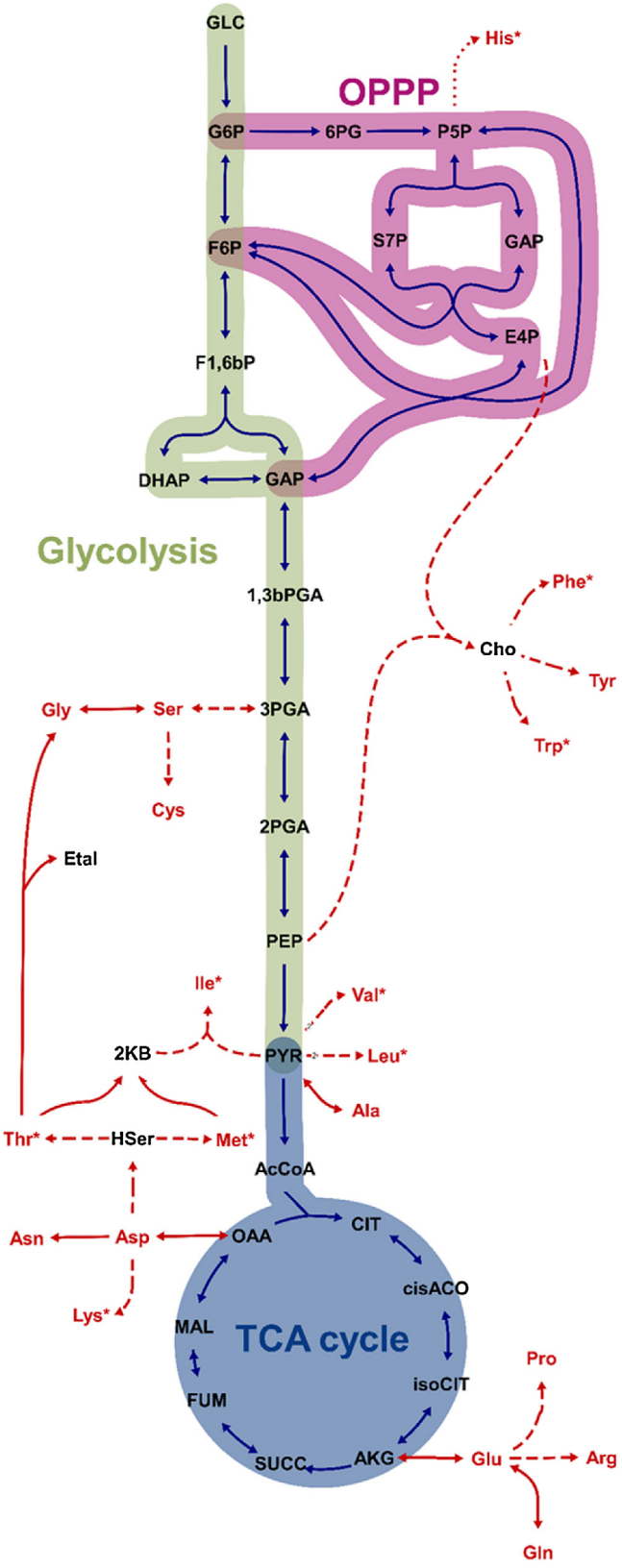

Fig. 1. Central metabolic pathways involved in amino acid biosynthesis. Pathways colored in green, pink and blue correspond to glycolysis, oxidative pentose phosphate pathway (OPPP) and tricarboxylic acid (TCA) cycle, respectively. Amino acids produced from the intermediates of these pathways are depicted in red. Asterisks (*) highlight the essential amino acids. Multiple- and single-step reactions involved in amino acid biosynthesis are depicted by dashed and solid arrows, respectively. The numbers adjacent to these arrows correspond to the number of precursor metabolites required for the synthesis of a particular amino acid.

essentially dependent on accurate assessment of metabolite MIDs [23].

The conventional approach does not quantify the labeling in free AAs but rather the proteinogenic ones through GC–MS [15,24–27] or NMR [28,29]. It is mainly because proteins are highly abundant than free AAs. However, proteinogenic AAs have much slower turnover and they are not suitable for studying the transient metabolism [30]. Intracellular AAs, on the other hand, reach metabolic steady-state much faster (5-fold) compared to proteinogenic AAs and they can reflect the instantaneous biochemistry of the cell [31,32]. Moreover, there are several drawbacks in determining MIDs of proteinogenic AAs by GC–MS: i.) the hydrolysis of the proteins results in degradation of several AAs including Trp, Gln, Asn and Cys; ii.) the derivativatized AAs are unstable; iii.) the GC–MS run commonly takes between 45 and 90 min. In order to circumvent aforementioned issues regarding analysis of proteinogenic AAs, recent studies have demonstrated the potential of more direct approach, which involves measuring MIDs of free AAs through MS-based techniques [23,33,34]. Iwatani et al., compared the accuracy of MIDs resulting from proteinogenic AAs and intracellular AA analyses through LC–MS/MS [33]. The study revealed that the method was inaccurate for free AAs at low abundances (Met and Trp), bivalent (His, Arg, Lys and Cys), and isomers (Leu/Ile) were not separated.

Towards improving the measurement of labeling enrichment of intracellular AAs for ^{13}C MFA, this work establishes a novel LC–MS/MS method using scheduled multiple reaction monitoring (MRM). The MIDs of all free AAs (except Trp) were rapidly assessed without the need of derivatization. Finally, this approach was tested and validated on free AAs extracted from maize embryos cultured with unlabeled substrates, ^{13}C-glucose or ^{13}C-glutamine; although Cys was below the limit of detection in these biological samples, the MIDs of a total of 18 free AAs were successfully determined.

2. Material and methods

2.1. Chemicals

The AA standards were obtained from Sigma-Aldrich (St. Louis, MO). [U-^{13}C]glucose, [1,2-^{13}C]glucose, and [U-^{13}C]glutamine were purchased from Isotec (Miamisburg, OH). Cation exchange resin (DOWEX 50WX8, 100–200 mesh), hydrochloric acid (HCl), sodium hydroxide, and LC–MS grade acetonitrile and acetic acid were ordered through ThermoFisher (Pittsburg, PA).

2.2. Biological material

Maize plants (*Zea mays* L.) were grown in a greenhouse as previously described [17]. Dissection and *in vivo* cultures of maize embryos grown in the presence of [U-^{13}C]glucose and [1,2-^{13}C]glucose or [U-^{13}C]glutamine were carried out following a published protocol [35].

Abbreviations of other metabolites in these pathways: GLC, glucose; G6P, glucose 6-phosphate; F6P, fructose 6-phosphate; 6PG, 6-phosphogluconic acid; P5P, pentose 5-phosphate; S7P, sedoheptulose 7-phosphate; GAP, glyceraldehyde 3-phosphate; E4P, erythrose 4-phosphate; F1,6bP, fructose 1,6-bisphosphate; DHAP, dihydroxyacetone phosphate; 1,3bPGA, 1,3-bisphosphoglycerate; 3PGA, 3-phosphoglycerate; 2PGA, 2-phosphoglycerate; Etal, acetaldehyde; Cho, chorismate; PEP, phosphoenolpyruvate; PYR, pyruvate; 2KB, 2-ketobutyrate; HSer, homoserine; AcCoA, acetyl-CoA; CIT, citrate; cisACO, *cis*-aconitate; isoCIT, isocitrate; AKG, α-ketoglutarate; SUCC, succinate; FUM, fumarate; MAL, malate; OAA, oxaloacetate.

Table 1
Specific amino acid-dependent MS parameters used for LC–MS/MS.

Amino acid	Parent ion formula	Daughter ion formula	Parent/daughter transition	DP*(V)	EP¶(V)	CE#(V)	CXP§(V)
Ala	$C_3H_8NO_2^+$	$C_2H_6N^+$	90.0/44.0	51	10	17	10
Arg	$C_6H_{15}N_4O_2^+$	$C_4H_8N^+$	175.0/70.0	60	10	33	10
Asn	$C_4H_9N_2O_3^+$	$C_2H_4NO_2^+$	133.0/74.0	80	10	21	12
Asp	$C_4H_8NO_4^+$	$C_2H_4NO_2^+$	134.0/74.0	45	10	21	10
Cys	$C_3H_8NO_2S^+$	$C_2H_3S^+$	122.0/59.0	100	10	29	10
Glu	$C_5H_{10}NO_4^+$	$C_4H_6NO^+$	148.0/84.0	31	10	23	12
Gln	$C_5H_{11}N_2O_3^+$	$C_4H_6NO^+$	147.0/84.0	40	10	24	12
Gly	$C_2H_6NO_2^+$	CH_4N^+	76.0/30.0	20	10	19	12
His	$C_6H_{10}N_3O_2^+$	$C_5H_8N_3^+$	156.0/110.0	50	10	21	16
Ile	$C_6H_{14}NO_2^+$	$C_5H_{12}N^+$	132.0/86.1	40	10	15	9
Leu	$C_6H_{14}NO_2^+$	$C_5H_{12}N^+$	132.0/86.1	40	10	15	9
Lys	$C_6H_{15}N_2O_2^+$	$C_5H_{10}N^+$	147.0/84.0	40	10	24	12
Met	$C_5H_{12}NO_2S^+$	$C_3H_6N^+$	150.0/56.1	45	10	23	8
Phe	$C_9H_{12}NO_2^+$	$C_8H_{10}N^+$	166.0/120.0	60	10	19	16
Pro	$C_5H_{10}NO_2^+$	$C_4H_8N^+$	116.0/70.0	56	10	23	10
Ser	$C_3H_8NO_3^+$	$C_2H_6NO^+$	106.0/60.0	31	10	15	10
Thr	$C_4H_{10}NO_3^+$	$C_3H_6N^+$	120.0/56.0	41	10	23	10
Trp	$C_{11}H_{13}N_2O_2^+$	$C_9H_8NO^+$	205.0/145.8	30	10	15	10
Tyr	$C_9H_{12}NO_3^+$	$C_7H_7^+$	182.0/91.0	51	10	19	16
Val	$C_5H_{12}NO_2^+$	$C_4H_{10}N^+$	118.0/72.0	30	10	22	8

*Declustering potential; ¶Entrance potential; #Collision energy; §Collision cell exit potential.

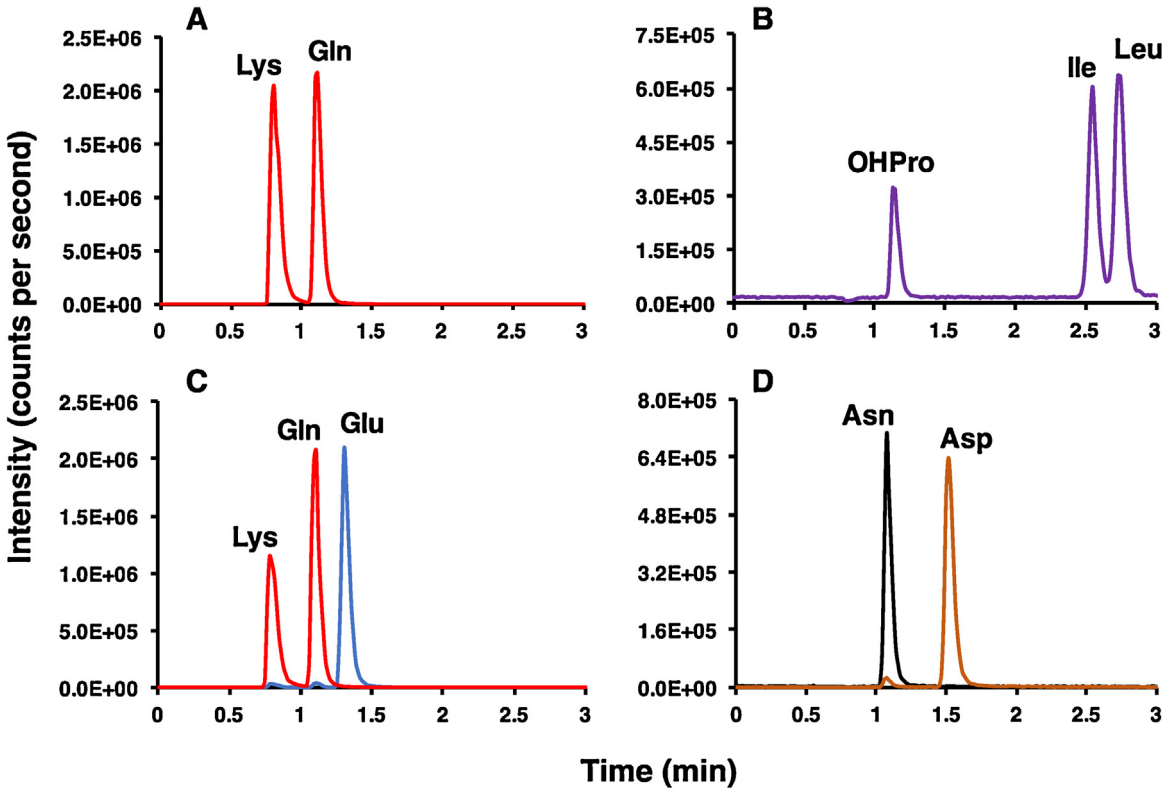

Fig. 2. Chromatographic resolution of isomers and natural heavy isotopomers of amino acids using MRM. Separation of **(A)** Lys and Gln (*m/z* 147.0/84.0), and **(B)** OHPro, Ile, Leu (*m/z* 132.0/86.1) isomers. Resolution of **(C)** Gln and Lys (*m/z* 147.0/84.0) naturally occurring heavy isotopomers, from Glu (*m/z* 148.0/84.0), and **(D)** Asn (*m/z* 133.0/74.0) naturally occurring heavy isotopomer from Asp (*m/z* 134.0/74.0). OHPro: hydroxyproline.

2.3. AA extraction and purification

Free AAs from maize embryos were extracted using boiling water [36,37], and then purified following an approach previously described [38] with some modifications. In brief, the lyophilized fraction of AAs was resuspended in 1 mL of 0.01 N HCl and loaded through a cation exchange resin (Dowex 50WX8, 100–200 mesh). The resin was washed with 5 mL of ultrapure water to remove the neutral and negatively charged molecules, and the retained free AAs were eluted using 5 mL of 1 N ammonium hydroxide. The collected fraction was placed under a stream of nitrogen at 60 °C until neutral pH, and then lyophilized overnight at −83 °C after being flash-frozen in liquid nitrogen. After lyophilization, the AA extracts were resuspended in 300 μL of ultrapure water, vortexed and transferred to a 3 kDa Amicon filtering device. The samples were centrifuged at 14,000*g* for 45 min at 4 °C and the resulting eluents (AAs) were

Table 2
Matrix effect (%), intra- and interday accuracy (%) of the 20 amino acids. Low accuracies are highlighted in bold.

		Accuracy (%)					
		Intraday assay (n = 4)			Interday assay (n = 12)		
AA	ME (%)*	0.25 μM¶	0.5 μM¶	1 μM¶	0.25 μM¶	0.5 μM¶	1 μM¶
Ala	99.1 ± 9.4	−12.7	−5.4	−0.8	−19.8	−10.2	−4.8
Arg	99.2 ± 7.7	−7.3	4.5	4.5	−10.0	0.9	−4.9
Asn	100.9 ± 5.2	−2.4	11.1	5.7	−2.6	1.8	−1.0
Asp	115.9 ± 13.8	2.3	−4.5	−7.0	−4.7	−4.0	−4.8
Cys	93.1 ± 1.3	−0.4	4.6	−3.1	2.0	9.0	5.6
Glu	98.4 ± 4.2	−8.5	14.9	0.9	−7.0	−3.2	−1.5
Gln	103.5 ± 2.8	−16.2	17.9	1.4	−15.6	−1.5	−1.6
Gly	87.7 ± 0.7	−7.4	−0.7	−3.7	−8.9	−3.6	−5.3
His	92.5 ± 4.8	−1.8	3.8	−4.1	−5.0	0.3	−2.9
Ile	98.6 ± 1.2	−1.0	11.9	−0.7	−0.2	0.0	0.2
Leu	97.6 ± 2.6	−0.5	9.0	0.5	−0.9	−0.7	1.1
Lys	106.3 ± 14.1	−6.3	1.9	−3.4	−8.3	4.6	−8.0
Met	97.7 ± 1.8	−2.9	8.6	−1.6	1.1	2.7	−2.4
Phe	99.4 ± 2.4	−8.2	8.5	0.4	−8.9	−2.4	−5.4
Pro	110.3 ± 16.8	−2.1	5.8	15.8	1.8	5.0	12.2
Ser	87.3 ± 14.3	−30.3	**33.8**	0.0	**−41.3**	4.3	−3.5
Thr	94.0 ± 5.6	−1.0	18.7	4.9	0.3	6.1	−1.6
Trp	100.4 ± 0.6	−1.9	9.4	1.6	−0.3	2.4	−1.9
Tyr	101.4 ± 0.2	0.0	9.7	1.1	0.2	0.7	−0.9
Val	99.2 ± 3.4	−2.6	9.8	5.0	−1.9	−4.9	0.5

*Matrix effect.
¶AA concentration added to maize embryo extract.

ready for LC–MS/MS analysis. 10 μL of AAs extracts from unlabeled or ^{13}C-labeled maize embryos were added to a LC–MS vial containing 1 mM of HCl, with a final volume of 1 mL.

2.4. Instrumentation and method development

The analysis of unlabeled and ^{13}C-labeled AAs was carried out using a UHPLC (Ultra High Pressure Liquid Chromatography) 1290 from Agilent Technologies, Inc (Santa Clara, CA) coupled to a hybrid Triple Quadrupole/Ion trap mass spectrometer QTRAP 5500 from AB Sciex (Framingham, MA). The AA extracts were placed in an autosampler kept at 15 °C. 5 μL of sample were injected onto the column. The liquid chromatography analysis was carried out at 30 °C. AAs were separated using a C18 Symmetry column (4.6 × 75 mm; 3.5 μm) with a Symmetry C18 pre-column (3.9 × 20 mm; 5 μm) from Waters (Milford, MA). The gradient used to separate the AAs consisted of acetonitrile plus 0.1% acetic acid (solvent A) and 0.1% acetic acid in water (solvent B). The total LC–MS/MS run was 11 min with a flow rate of 800 μL/min. The gradient was applied as follows: A = 0–2 min 0%, 2–6.5 min 20%, 6.5–6.6 min 80%, 6.6–8.5 min 80%, 8.5–8.6 min 0%, 8.6–11 min 0%.

The mass spectra were acquired using electrospray ionization in a positive mode. The AAs were detected in the same LC–MS/MS run using multiple reaction monitoring (MRM). The source parameters such as curtain gas (30 psi), ionization (2500 V), temperature (650 °C), nebulizer gas (60 psi), heating gas (60 psi), and collision activated dissociation (Medium) were kept constant for MRM and scheduled MRM. The mass spectrometer was set to have a dwell time of 30 msec for the MRM scan survey whereas a 40 s scanning window was defined for each AA using scheduled MRM. The declustering (DP), entrance (EP), collision energy (CE), and collision cell exit (CXP) potentials for each metabolite are reported in Table 1. LC–MS/MS data were acquired and processed using Analyst 1.6.1 software.

2.5. Determination of matrix effect and accuracy intra- and inter-assay

Matrix effect (ME) for the twenty AAs was determined using four biological maize extracts which were spiked, after extraction, with a known concentration of a mixture containing external amino acid standards (1 μM for each AA). The ion suppression by the biological matrix was calculated in a percentage with an equation of ME (%) = 100 × [peak area (sample spiked after extraction) – peak area (sample)]/mean peak area (AA external standard).

The intra-assay for accuracy was assessed for the 20 AAs using four maize biological samples and three different concentrations (0.25, 0.5, and 1.0 μM) of a mixture of external amino acid standards. The accuracy inter-assay was achieved using the three concentration of AA external standard mentioned previously in four replicates on three different days. The accuracy was defined as the relative mean error (RME) in percentage, using the following equation: RME (%) = 100 × [(mean measured AA concentration – theoretical AA concentration)/theoretical AA concentration]. Note that the area of each AA present in the biological maize sample was subtracted prior to calculation of the accuracy.

2.6. Raw data processing and isotopomer calculation

After acquisition of the data, the intensity (height) of the different transitions (parent/daughter ions) corresponding to each AA was integrated manually and transferred to an excel file after background subtraction. Then, the transitions associated with one isotopomer were summed, and the isotopomer abundance for each AA was calculated by dividing the intensity of a particular isotopomer by the sum of all isotopomers.

2.7. Correction for natural abundance

Following isotopomer calculation, AAs were corrected for natural abundance of isotope using Scilab an open source software (www.scilab.org) in order to measure the labeling enrichment of each AA.

3. Results and discussion

3.1. LC–MS/MS method development for AA quantification

AAs are zwitterionic, meaning that they have both positive and negative charges at physiological pH. The addition of organic acids,

Table 3
^{13}C-labeled AA isotopomers monitoring using scheduled MRM and their mass isotopomer distributions (MIDs) in ^{13}C-labeled samples. ¶Retention time; #Mass isotopomers.

AA	RT¶(min)	MI#	Parent/daughter transition	[^{13}C]Gln Average ± SD	[^{13}C]Glc Average ± SD
Ala	1.12	m_0	90/44	0.970 ± 0.003	0.702 ± 0.010
		m_1	91/44; 91/45	0.027 ± 0.001	0.076 ± 0.004
		m_2	92/45; 92/46	−0.002 ± 0.001	0.144 ± 0.003
		m_3	93/46	0.004 ± 0.001	0.080 ± 0.003
Arg*	0.87	m_0	175/60	0.710 ± 0.038	0.432 ± 0.011
		m_1	176/60; 176/61	0.103 ± 0.021	0.218 ± 0.007
		m_2	177/60; 177/61	0.001 ± 0.005	0.195 ± 0.005
		m_3	178/60; 178/61	0.060 ± 0.013	0.100 ± 0.002
		m_4	179/60; 179/61	0.000 ± 0.001	0.040 ± 0.001
		m_5	180/60; 181/61	0.127 ± 0.003	0.014 ± 0.001
		m_6	181/61	−0.001 ± 0.002	0.002 ± 0.001
Asn	1.11	m_0	133/74	0.879 ± 0.012	0.549 ± 0.012
		m_1	134/74; 134/75	0.068 ± 0.002	0.192 ± 0.006
		m_2	135/74; 135/75; 135/76	0.017 ± 0.003	0.161 ± 0.011
		m_3	136/75; 136/76	0.006 ± 0.003	0.081 ± 0.006
		m_4	137/76	0.031 ± 0.010	0.018 ± 0.001
Asp*	1.60	m_0	134/88	0.852 ± 0.029	0.507 ± 0.005
		m_1	135/88; 135/89	0.077 ± 0.020	0.197 ± 0.002
		m_2	136/89; 136/90	0.018 ± 0.006	0.190 ± 0.008
		m_3	137/90; 137/91	0.011 ± 0.003	0.085 ± 0.005
		m_4	138/91	0.043 ± 0.012	0.022 ± 0.001
Cys*	1.16	m_0	122/76	nd	nd
		m_1	123/76; 123/77	nd	nd
		m_2	124/77; 124/78	nd	nd
		m_3	125/78	nd	nd
Glu	1.35	m_0	148/84	0.759 ± 0.021	0.458 ± 0.009
		m_1	149/84; 149/85	0.070 ± 0.004	0.162 ± 0.005
		m_2	150/85; 150/86	0.014 ± 0.002	0.245 ± 0.008
		m_3	151/86; 151/87	0.037 ± 0.004	0.085 ± 0.001
		m_4	152/87; 152/88	0.008 ± 0.001	0.039 ± 0.001
		m_5	153/88	0.115 ± 0.011	0.011 ± 0.000
Gln*	1.12	m_0	147/130	0.688 ± 0.044	0.498 ± 0.003
		m_1	148/131	0.064 ± 0.005	0.150 ± 0.001
		m_2	149/132	0.017 ± 0.004	0.226 ± 0.002
		m_3	150/133	0.040 ± 0.008	0.079 ± 0.001
		m_4	151/134	0.011 ± 0.002	0.037 ± 0.001
		m_5	152/135	0.182 ± 0.025	0.011 ± 0.000
Gly	1.04	m_0	76/30	0.960 ± 0.028	0.711 ± 0.007
		m_1	77/30; 77/31	0.040 ± 0.025	0.205 ± 0.013
		m_2	78/31	0.000 ± 0.003	0.086 ± 0.019
His*	0.86	m_0	156/93	0.946 ± 0.005	0.446 ± 0.013
		m_1	157/93; 157/94	0.054 ± 0.004	0.252 ± 0.006
		m_2	158/94; 158/95	−0.003 ± 0.002	0.160 ± 0.006
		m_3	159/95; 159/96	0.000 ± 0.000	0.073 ± 0.008
		m_4	160/96; 160/97	0.001 ± 0.001	0.042 ± 0.001
		m_5	161/97; 161/98	0.003 ± 0.003	0.023 ± 0.004
		m_6	162/98	0.000 ± 0.001	0.004 ± 0.002
Ile	2.55	m_0	132/86	0.898 ± 0.005	0.371 ± 0.006
		m_1	133/86; 133/87	0.073 ± 0.002	0.121 ± 0.002
		m_2	134/87; 134/88	0.027 ± 0.004	0.318 ± 0.007
		m_3	135/88; 135/89	0.002 ± 0.002	0.068 ± 0.004
		m_4	136/89; 136/90	0.000 ± 0.001	0.101 ± 0.003
		m_5	137/90; 137/91	0.000 ± 0.000	0.010 ± 0.001
		m_6	138/91	0.000 ± 0.000	0.010 ± 0.001
Leu	2.77	m_0	132/86	0.870 ± 0.015	0.440 ± 0.006
		m_1	133/86; 133/87	0.088 ± 0.005	0.175 ± 0.001
		m_2	134/87; 134/88	0.012 ± 0.002	0.218 ± 0.005
		m_3	135/88; 135/89	0.005 ± 0.004	0.100 ± 0.003
		m_4	136/89; 136/90	0.025 ± 0.006	0.048 ± 0.002
		m_5	137/90; 137/91	0.001 ± 0.000	0.016 ± 0.001
		m_6	138/91	0.000 ± 0.000	0.004 ± 0.000
Lys	0.84	m_0	147/84	0.873 ± 0.018	0.444 ± 0.017
		m_1	148/84; 148/85	0.079 ± 0.008	0.166 ± 0.004
		m_2	149/85; 149/86	0.013 ± 0.005	0.217 ± 0.009
		m_3	150/86; 150/87	0.021 ± 0.005	0.113 ± 0.007
		m_4	151/87; 151/88	0.015 ± 0.003	0.047 ± 0.002
		m_5	152/88; 152/89	0.000 ± 0.000	0.012 ± 0.001
		m_6	153/89	0.000 ± 0.000	0.003 ± 0.001

Table 3 (*Continued*)

AA	RT[¶](min)	MI[#]	Parent/daughter transition	[^{13}C]Gln Average ± SD	[^{13}C]Glc Average ± SD
Met[*]	1.91	m_0	150/104	0.890 ± 0.005	0.488 ± 0.005
		m_1	151/104;151/105	0.073 ± 0.008	0.274 ± 0.006
		m_2	152/105; 152/106	0.003 ± 0.007	0.130 ± 0.012
		m_3	153/106; 153/107	0.019 ± 0.000	0.078 ± 0.018
		m_4	154/107; 154/108	0.016 ± 0.006	0.030 ± 0.003
		m_5	155/108	−0.001 ± 0.001	0.002 ± 0.002
Phe	5.0	m_0	166/120	0.905 ± 0.002	0.320 ± 0.008
		m_1	167/120; 167/121	0.090 ± 0.002	0.150 ± 0.004
		m_2	168/121; 168/122	0.002 ± 0.001	0.218 ± 0.004
		m_3	169/122; 169/123	0.001 ± 0.001	0.149 ± 0.002
		m_4	170/123; 170/124	0.000 ± 0.001	0.083 ± 0.004
		m_5	171/124; 171/125	0.000 ± 0.000	0.049 ± 0.002
		m_6	172/125; 172/126	0.000 ± 0.000	0.021 ± 0.000
		m_7	173/126; 173/127	0.000 ± 0.000	0.007 ± 0.001
		m_8	174/127; 174/128	0.000 ± 0.000	0.002 ± 0.000
		m_9	175/128	0.000 ± 0.000	0.001 ± 0.000
Pro	1.26	m_0	116/70	0.823 ± 0.010	0.758 ± 0.010
		m_1	117/70; 117/71	0.035 ± 0.002	0.073 ± 0.004
		m_2	118/71; 118.0/72	0.008 ± 0.002	0.111 ± 0.003
		m_3	119/72; 119/73	0.024 ± 0.002	0.037 ± 0.003
		m_4	120/73; 120/74	0.005 ± 0.001	0.017 ± 0.001
		m_5	125/74	0.106 ± 0.008	0.005 ± 0.000
Ser[*]	1.06	m_0	106/88	0.897 ± 0.009	0.597 ± 0.004
		m_1	107/89	0.052 ± 0.006	0.177 ± 0.006
		m_2	108/90	0.016 ± 0.004	0.140 ± 0.008
		m_3	109/91	0.036 ± 0.009	0.088 ± 0.011
Thr[*]	1.09	m_0	120/74	0.898 ± 0.012	0.557 ± 0.009
		m_1	121/74; 121/75	0.065 ± 0.006	0.190 ± 0.001
		m_2	122/75; 122/76	0.008 ± 0.002	0.154 ± 0.008
		m_3	123/76; 123/77	0.005 ± 0.001	0.080 ± 0.005
		m_4	124/77	0.024 ± 0.003	0.020 ± 0.001
Tyr[*]	3.21	m_0	182/136	0.899 ± 0.002	0.297 ± 0.007
		m_1	183/136; 183/137	0.096 ± 0.002	0.158 ± 0.002
		m_2	184/137; 184/138	0.002 ± 0.001	0.222 ± 0.003
		m_3	185/138; 185/139	0.000 ± 0.000	0.145 ± 0.003
		m_4	186/139; 186/140	0.000 ± 0.000	0.092 ± 0.002
		m_5	187/140; 187/141	0.002 ± 0.002	0.052 ± 0.001
		m_6	188/141; 188/142	0.000 ± 0.000	0.023 ± 0.001
		m_7	189/142; 189/143	0.000 ± 0.000	0.008 ± 0.001
		m_8	190/143; 190/144	0.000 ± 0.000	0.002 ± 0.001
		m_9	191/144	0.000 ± 0.000	0.001 ± 0.000
Val	1.47	m_0	118/72	0.825 ± 0.012	0.456 ± 0.009
		m_1	119/72; 119/73	0.075 ± 0.005	0.146 ± 0.001
		m_2	120/73; 120/74	0.016 ± 0.002	0.251 ± 0.004
		m_3	121/74; 121/75	0.083 ± 0.006	0.090 ± 0.002
		m_4	122/75; 122/76	0.000 ± 0.000	0.039 ± 0.002
		m_5	123/76	0.000 ± 0.000	0.018 ± 0.001

[*]Due to contaminants in one or more parent/daughter pairs, new isotopomer transitions were tested and validated. The parameters for these alternative transitions are reported in Table A2 (Supplementary Material) and the isotopomer distributions for each AA are shown in Table A3 (Supplementary Material). No suitable parent/daughter pairs were found for Trp. Average and standard deviation (SD) of three biological replicates are reported for steady-state MIDs of ^{13}C-labeled AAs from maize embryos incubated with [^{13}C]glutamine ([^{13}C]Gln) or [^{13}C]glucose ([^{13}C]Glc). "nd" refers to AAs for which MIDs were not determined due to low abundance.

such as acetate, in the mobile phase stabilizes the positive charge of the amine group of the AAs, which allows their monitoring in positive mode. Using this approach, the separation of the 20 AAs was achieved with a reverse phase C18 Symmetry column (4.6 × 75 mm; 3.5 μm). A triple quadrupole AB Sciex QTRAP 5500 was used in positive ion mode, and multiple reaction monitoring (MRM) allowed simultaneous detection of the 20 AAs. For this purpose, MS parameters (DP, EP, CE, and CXP) were optimized for each transition using AB Sciex Analyst 1.6.1 software, and the most abundant daughter ion for each AA is reported in Table 1. Except Met and Tyr, these daughter ions were also found to be the most abundant in other studies [39,40]. A gradient of acetonitrile was applied to separate the AAs while acetic acid was maintained at 0.1% throughout the 11 min run. The initial conditions were 0% acetonitrile for two minutes, which allowed the elution of 15 AAs. Then, the acetonitrile gradient was linearly increased to 20% for 4.5 min to elute the remaining AAs. Finally, the column was washed with 80% acetonitrile for 2 min, and original conditions were restored for 2.5 min. The separation of the 20 AAs was accomplished in less than 7 min (Table A1, Supplementary Material). Importantly, the chromatographic resolution of: i) the pairs of isomers Ile/Leu (132.0/86.1), and Lys/Gln (147.0/84.0), and ii) naturally occurring heavy isotopomers Gln (147.0/84.0) from Glu (148.0/84.0), and Asn (133.0/74.0) from Asp (134.0/74.0), was completely achieved (Fig. 2A-D). Additionally, this method is extremely sensitive: the limits of detection (LOD) and quantification (LOQ) were calculated and ranged from 0.3 to 32.3 fmol and 1.1 to 108.0 fmol, respectively (Table A1, Supplementary Material). The calibration curve of each AA displayed excellent linearity from 20 to 50,000 fmol ($r^2 > 0.9835$). To further validate the method, the matrix effect (ME) for each amino acid was investigated as well as the accuracy intra- and inter-assay. Overall, little or no ME was observed for the 20

AAs as shown in Table 2, demonstrating that there was no ion suppression due to the matrix of the sample, even for the AA eluting in the void volume. Hence, this method will not require the addition of ion pairing agents which are usually used to circumvent ion suppression from a biological sample by improving metabolite retention [39–43]. Finally, the accuracy intra- and inter-assay was assessed as described in the Material and Methods, and found to be in the ± 20% allowance range except for Ser which had a relative mean error (RME) of ± 30% (Table 2).

3.2. LC–MS/MS method validation for quantification of the AAs labeling

In order to validate the LC–MS/MS method to accurately measure isotopomer distributions, the naturally occurring isotopes (aka unlabeled atoms) can be used [14]. A mix of unlabeled AA standards was analyzed through LC–MS/MS using scheduled MRM based on the retention time of each AA. The number of transitions for an AA containing n carbon atoms was n + 1, 2n or 3(n-1) for neutral losses of zero, one or two carbons, respectively (Tables 1 and 3). First, the fractional abundance of each isotopomer of a given AA was determined by the ratio of the corresponding ion count (peak intensity) to the total ion count of all fractions. The resulting values were then corrected for natural abundances using Scilab, an open source software. For the accurate reflection of the theoretical distribution of naturally occurring isotopes, absolute error should be less than 1.5% or 0.985 for M_0 [44]. From analysis of AA standards, ten AAs had values close to 1 (100% unlabeled) for M_0 isotopomers (Table A3, Supplementary Material). For those that did not correct (<0.985 for M_0) for natural abundances due to contaminants, alternative parent/daughter ion pairs were tested, which resulted in values close to 1. Such AAs are denoted by asterisks in Table 3, and the optimal parameters for MID determination are reported in Table A2 (Supplementary Material). The alternative parent/daughter ion pairs resulted in significant loss of sensitivity, by a factor 2–6, for Ser, His and Arg (Table A2, Supplementary Material). Tryptophan was the only AA for which no suitable parent/daughter ion pair was found. Therefore, Trp was omitted from further analyses. Additionally, cysteine was found to be below the limit of detection in maize embryos (Table 3). This phenomenon is explained by the conversion of cysteine into cystine due to extraction with boiling water and purification through cation exchange resin (Fig. A1A -B, Supplementary Material).

3.3. LC–MS/MS method application: assessing MIDs of ^{13}C-labeled samples

Maize embryos were incubated with either a mixture of 20% [U-^{13}C]glucose and 80%[1,2-^{13}C]glucose, or 100% [U-^{13}C]glutamine until isotopic steady state was attained [35]. Intracellular AAs were extracted as previously described [36,37], and purified through a cation exchange resin as explained in the experimental section. Purified ^{13}C-AAs were then analyzed through LC–MS/MS using scheduled MRM. From each labeling experiment (with [^{13}C]-glucose and with [^{13}C]-glutamine) mass isotopomers of 19 AAs were determined using the parent/daughter transitions listed in Table 3. As previously noted, the fractional abundance of each isotopomer was calculated relative to the sum of all isotopomers. Then, the resulting values were corrected for natural abundances of all atoms except for carbons. For each labeling experiment, a total of four biological replicates were analyzed and the average values for mass isotopomer abundances are reported in Table 3. However, cysteine was found to be below the limit of detection in maize embryos. At metabolic steady-state, the ^{13}C-labeling decreases as the AAs are further away from the labeling entry point. Labeled glutamine enters metabolism at the level of the TCA cycle, which is particularly appropriate to define the lower part of the metabolic map (Fig. 1). One of the major findings from glutamine labeling is that His MID was close to the natural abundance (Table 3), highlighting a gluconeogenic flux null or extremely low in developing maize embryos, which is in accordance with a previous study [17]. When using 80% [1,2-^{13}C]glucose and 20% [U-^{13}C]glucose, all the AAs were labeled at metabolic steady-state. Interestingly, a large proportion of histidine was found to be labeled in one carbon, revealing the action of the OPPP: this pathway released the first carbon of the hexose-phosphates as CO_2.

4. Conclusion

In this work, a high-throughput LC–MS/MS method was developed and validated to quantify the levels and the labeling abundances of free AAs in biological samples. To our knowledge, this is the first study that allows the complete measurements of MIDs of the highest number of free AAs (19) without using derivatization. Although this technical advance was validated on maize embryos at metabolic steady-state, it is fully applicable to dynamic labeling experiments, and to various organisms and tissues. We anticipate that this novel methodology that allows the direct measurement of MIDs in free AAs will improve the resolution and precision of carbon fluxes through central metabolism.

Acknowledgements

The authors thank the Targeted Metabolomics Laboratory (metabolomics.osu.edu) at The Ohio State University for access to the LC–MS/MS equipment, funded by the Translational Plant Sciences Targeted Investment in Excellence (TIE). We also would like to thank Gary Posey (Greenhouse superintendent). J.C.C was supported in part by the Agriculture and Food Research Initiative competitive grant # 2016-67013-24605 from the USDA National Institute of Food and Agriculture. E.T was supported in part by the DOE Office of Science, Office of Biological and Environmental Research (BER), grant # DE-SC0016490.

Appendix A. Supplementary data

Supplementary data associated with this article can be found, in the online version, at http://dx.doi.org/10.1016/j.chroma.2017.02.028.

References

[1] H.E. Umbarger, Amino acid biosynthesis and its regulation, Annu. Rev. Biochem. 47 (1978) 532–606.
[2] B. Alberts, A. Johnson, J. Lewis, D. Morgan, M. Raff, K. Roberts, P. Walter, Molecular biology of the cell, sixth edition, in: Molecular Biology of the Cell, sixth edition, 2015, pp. 1–1342.
[3] J.M. Berg, Biochemistry, revised edition, Chem. Eng. News 79 (2001), 130–130.
[4] T. Huang, G. Jander, M. de Vos, Non-protein amino acids in plant defense against insect herbivores: representative cases and opportunities for further functional analysis, Phytochemistry 72 (2011) 1531–1537.
[5] N. Dudareva, A. Klempien, J.K. Muhlemann, I. Kaplan, Biosynthesis, function and metabolic engineering of plant volatile organic compounds, New Phytol. 198 (2013) 16–32.
[6] J. Furstenberg-Hagg, M. Zagrobelny, S. Bak, Plant defense against insect herbivores, Int. J. Mol. Sci. 14 (2013) 10242–10297.
[7] R.B. Herbert, The biosynthesis of plant alkaloids and nitrogenous microbial metabolites, Nat. Prod. Rep. 20 (2003) 494–508.
[8] J.K. Weng, C. Chapple, The origin and evolution of lignin biosynthesis, New Phytol. 187 (2010) 273–285.
[9] S.C. Daubner, T. Le, S. Wang, Tyrosine hydroxylase and regulation of dopamine synthesis, Arch. Biochem. Biophys. 508 (2011) 1–12.
[10] S.B. Crown, M.R. Antoniewicz, Publishing 13C metabolic flux analysis studies: a review and future perspectives, Metab. Eng. 20 (2013) 42–48.
[11] M. Dieuaide-Noubhani, A.P. Alonso, Application of metabolic flux analysis to plants, Methods Mol. Biol. 1090 (2014) 1–18.

[12] U. Sauer, Metabolic networks in motion: 13C-based flux analysis, Mol. Syst. Biol. 2 (2006) 62.
[13] W. Wiechert, K. Noh, From stationary to instationary metabolic flux analysis, Adv. Biochem. Eng. Biotechnol. 92 (2005) 145–172.
[14] N. Zamboni, 13C metabolic flux analysis in complex systems, Curr. Opin. Biotechnol. 22 (2011) 103–108.
[15] Y. Toya, N. Ishii, K. Nakahigashi, T. Hirasawa, T. Soga, M. Tomita, K. Shimizu, 13C-metabolic flux analysis for batch culture of Escherichia coli and its Pyk and Pgi gene knockout mutants based on mass isotopomer distribution of intracellular metabolites, Biotechnol. Prog. 26 (2010) 975–992.
[16] L.M. Blank, F. Lehmbeck, U. Sauer, Metabolic-flux and network analysis in fourteen hemiascomycetous yeasts, FEMS Yeast Res. 5 (2005) 545–558.
[17] A.P. Alonso, V.L. Dale, Y. Shachar-Hill, Understanding fatty acid synthesis in developing maize embryos using metabolic flux analysis, Metab. Eng. 12 (2010) 488–497.
[18] A.P. Alonso, D.L. Val, Y. Shachar-Hill, Central metabolic fluxes in the endosperm of developing maize seeds and their implications for metabolic engineering, Metab. Eng. 13 (2011) 96–107.
[19] X.W. Chen, A.P. Alonso, D.K. Allen, J.L. Reed, Y. Shachar-Hill, Synergy between (13)C-metabolic flux analysis and flux balance analysis for understanding metabolic adaption to anaerobiosis in E. coli, Metab. Eng. 13 (2011) 38–48.
[20] E. Fischer, U. Sauer, Metabolic flux profiling of Escherichia coli mutants in central carbon metabolism using GC–MS, Eur. J. Biochem. 270 (2003) 880–891.
[21] J.W. Locasale, A.R. Grassian, T. Melman, C.A. Lyssiotis, K.R. Mattaini, A.J. Bass, G. Heffron, C.M. Metallo, T. Muranen, H. Sharfi, A.T. Sasaki, D. Anastasiou, E. Mullarky, N.I. Vokes, M. Sasaki, R. Beroukhim, G. Stephanopoulos, A.H. Ligon, M. Meyerson, A.L. Richardson, L. Chin, G. Wagner, J.M. Asara, J.S. Brugge, L.C. Cantley, M.G. Vander Heiden, Phosphoglycerate dehydrogenase diverts glycolytic flux and contributes to oncogenesis, Nat. Genet. 43 (2011) 869–U879.
[22] J.V. Sa, S. Kleiderman, C. Brito, U. Sonnewald, M. Leist, A.P. Teixeira, P.M. Alves, Quantification of metabolic rearrangements during neural stem cells differentiation into astrocytes by metabolic flux analysis, Neurochem. Res. 42 (2016) 244–253.
[23] J. Choi, M.T. Grossbach, M.R. Antoniewicz, Measuring complete isotopomer distribution of aspartate using gas chromatography/tandem mass spectrometry, Anal. Chem. 84 (2012) 4628–4632.
[24] T. Szyperski, Biosynthetically directed fractional 13C-labeling of proteinogenic amino acids. An efficient analytical tool to investigate intermediary metabolism, Eur. J. Biochem. 232 (1995) 433–448.
[25] M.R. Antoniewicz, J.K. Kelleher, G. Stephanopoulos, Accurate assessment of amino acid mass isotopomer distributions for metabolic flux analysis, Anal. Chem. 79 (2007) 7554–7559.
[26] A.P. Alonso, F.D. Goffman, J.B. Ohlrogge, Y. Shachar-Hill, Carbon conversion efficiency and central metabolic fluxes in developing sunflower (Helianthus annuus L.) embryos, Plant J. 52 (2007) 296–308.
[27] D.K. Allen, R.W. Laclair, J.B. Ohlrogge, Y. Shachar-Hill, Isotope labelling of Rubisco subunits provides in vivo information on subcellular biosynthesis and exchange of amino acids between compartments, Plant Cell Environ. 35 (2012) 1232–1244.
[28] Q. Truong, J.V. Shanks, Analysis of proteinogenic amino acid and starch labeling by 2D NMR, Methods Mol. Biol. 1090 (2014) 87–105.
[29] S. Massou, C. Nicolas, F. Letisse, J.C. Portais, NMR-based fluxomics: quantitative 2D NMR methods for isotopomers analysis, Phytochemistry 68 (2007) 2330–2340.
[30] F. Ma, L.J. Jazmin, J.D. Young, D.K. Allen, Isotopically nonstationary 13C flux analysis of changes in Arabidopsis thaliana leaf metabolism due to high light acclimation, Proc. Natl. Acad. Sci. U. S. A. 111 (2014) 16967–16972.
[31] N. Okahashi, S. Kajihata, C. Furusawa, H. Shimizu, Reliable metabolic flux estimation in escherichia coli central carbon metabolism using intracellular free amino acids, Metabolites 4 (2014) 408–420.
[32] E. Mori, C. Furusawa, S. Kajihata, T. Shirai, H. Shimizu, Evaluating C-13 enrichment data of free amino acids for precise metabolic flux analysis, Biotechnol. J. 6 (2011) 1377–1387.
[33] S. Iwatani, S. Van Dien, K. Shimbo, K. Kubota, N. Kageyama, D. Iwahata, H. Miyano, K. Hirayama, Y. Usuda, K. Shimizu, K. Matsui, Determination of metabolic flux changes during fed-batch cultivation from measurements of intracellular amino acids by LC-MS/MS, J. Biotechnol. 128 (2007) 93–111.
[34] M. Ruhl, B. Rupp, K. Noh, W. Wiechert, U. Sauer, N. Zamboni, Collisional fragmentation of central carbon metabolites in LC-MS/MS increases precision of 13C metabolic flux analysis, Biotechnol. Bioeng. 109 (2012) 763–771.
[35] M. Koubaa, J.-C. Cocuron, B. Thomasset, A.P. Alonso, Highlighting the tricarboxilic acid cycle: liquid and gas chromatography-mass spectrometry analyses of 13C-labeled organic acids, Anal. Biochem. 436 (2013) 151–159.
[36] J.C. Cocuron, A.P. Alonso, Liquid chromatography tandem mass spectrometry for measuring 13C-labeling in intermediaries of the glycolysis and pentose-phosphate pathway, Methods Mol. Biol. 1090 (2014) 131–142.
[37] J.C. Cocuron, B. Anderson, A. Boyd, A.P. Alonso, Targeted metabolomics of *Physaria fendleri*, an industrial crop producing hydroxy fatty acids, Plant Cell Physiol. 55 (2014) 620–633.
[38] R.J. Redgwell, Fractionation of plant-extracts using ion-exchange sephadex, Anal. Biochem. 107 (1980) 44–50.
[39] L. Gu, A.D. Jones, R.L. Last, LC-MS/MS assay for protein amino acids and metabolically related compounds for large-scale screening of metabolic phenotypes, Anal. Chem. 79 (2007) 8067–8075.
[40] K. Petritis, P. Chaimbault, C. Elfakir, M. Dreux, Parameter optimization for the analysis of underivatized protein amino acids by liquid chromatography and ionspray tandem mass spectrometry, J. Chromatogr. A 896 (2000) 253–263.
[41] P. Chaimbault, K. Petritis, C. Elfakir, M. Dreux, Determination of 20 underivatized proteinic amino acids by ion-pairing chromatography and pneumatically assisted electrospray mass spectrometry, J. Chromatogr. A 855 (1999) 191–202.
[42] P. Chaimbault, K. Petritis, C. Elfakir, M. Dreux, Ion-pair chromatography on a porous graphitic carbon stationary phase for the analysis of twenty underivatized protein amino acids, J. Chromatogr. A 870 (2000) 245–254.
[43] M. de Person, P. Chaimbault, C. Elfakir, Analysis of native amino acids by liquid chromatography/electrospray ionization mass spectrometry: comparative study between two sources and interfaces, J. Mass Spectrom. 43 (2008) 204–215.
[44] J.M. Buescher, M.R. Antoniewicz, L.G. Boros, S.C. Burgess, H. Brunengraber, C.B. Clish, R.J. DeBerardinis, O. Feron, C. Frezza, B. Ghesquiere, E. Gottlieb, K. Hiller, R.G. Jones, J.J. Kamphorst, R.G. Kibbey, A.C. Kimmelman, J.W. Locasale, S.Y. Lunt, O.D.K. Maddocks, C. Malloy, C.M. Metallo, E.J. Meuillet, J. Munger, K. Noh, J.D. Rabinowitz, M. Ralser, U. Sauer, G. Stephanopoulos, J. St-Pierre, D.A. Tennant, C. Wittmann, M.G. Vander Heiden, A. Vazquez, K. Vousden, J.D. Young, N. Zamboni, S.M. Fendt, A roadmap for interpreting C-13 metabolite labeling patterns from cells, Curr. Opin. Biotech. 34 (2015) 189–201.